Chalcogenide Letters Vol. 21, No. 3, March 2024, p. 285 - 291

Quantum size effects on PbSeS semiconductor quantum dots, an experimental and theoretical approach

M. I. Ahamed[a,*], T. Ayyasamy[b], N. Prathap[a], S. Ahamed[c]
[a]*Department of Electronics and Communication Engineering, E.G.S. Pillay Engineering College, Nagapattinam, Tamilnadu, India.*
[b]*Department of Aeronautical Engineering, Dhanalakshmi Srinivasan Engineering College (Autonomous), Perambalur, Tamilnadu, India.*
[c]*Department of Computer Science, College of Computer Science and Information Technology, Jazan University, Jazan, Kingdom of Saudi Arabia.*

In recent times, zero-dimensional materials have gained importance from a fundamental and technological perspective. Lead selenium sulphide (PbSeS) is a potential candidate for finding interest in its zero-dimensional form among many compound semiconductors. Hence, in this communication, we explored the impact of quantum confinement effects on the energy band gap and wavelength of PbSeS semiconductor nanocrystals (Quantum dots) using cohesive energy and hyperbolic band models (HBM). Experimental data, such as scanning electron microscopy, UV-Vis-NIR, and PL spectroscopies were used to determine the size of nanoparticles and wavelength. PbSeS nanocrystals were also prepared by one-pot synthesis. The experimental results showed that the prepared PbSeS nanostructures are formed with tiny nanometer size, which showed a redshift of about 0.79eV in energy bandgap. A theoretical study showed that the energy bandgap in quantum-sized PbSeS differs from that in its bulk crystal.

(Received December 1, 2023; Accepted March 25, 2024)

Keywords: PbSeS, Quantum dots, Cohesive energy, Hyperbolic band model, Solar cell

1. Introduction

Materials at the nanoscale are expected to possess different physical properties than their bulk counterparts. It is essential to pay attention to semiconductor quantum dots (QDs); QDs are tiny, trifling structures (ranging in size from 1 to 10 nm), such as semiconductor-made nanocrystals implanted in an alternative semiconductor-based material. Based on their electronic physiologies, electrons can be contained in all three dimensions based on their shape and size [1-3]. Since the early 1990s, QDs have been widely used for various remarkable applications. Optoelectronic properties are typically the basis of most advanced contemporary machines. Using their ability to absorb, emit, convert, and detect light daily, they can fulfill a wide range of innovative daily applications and have become increasingly controllable and accustomed to society's needs. According to L.E. Brus at Columbia University, systematic progress was determined by the remarkable science and technology of QDs. Based on semiconductor base nanoparticles, Brus derived the relationship between size and energy bandgap, which links sphere model approximations with bulk semiconductor wave function ideologies [4-5].

In light of the fact that QDs are anticipated to play a vital role in optoelectronic devices. One of the most noteworthy aspects of QDs is their ability to emit light covering the visible and the infrared spectrum. Thus, it is an ideal material for various optical devices. Recent years have seen a surge in the demand for green nanotechnology innovations. Recently, QD solar cells have been shown to provide a critical solution [6-8]. The intermediate energy band will be created if QDs are piled up densely in three dimensions like an artificial crystal. QDs' intermediate band is predicted to have a photoelectric conversion efficiency above 70%, several times that of current silicon-based solar cells [9].

* Corresponding author: irshad_bcet@yahoo.co.in
https://doi.org/10.15251/CL.2024.213.285

IV-VI group materials have received more attention due to their diverse applications among semiconductors. In group IV-VI semiconductors, lead chalcogenides occupy a unique position. The narrow energy bandgap of lead chalcogenides is one of their most intriguing features. Due to the small effective masses of holes and electrons in lead chalcogenides, they exhibit an extensive wavelength range, ranging from UV to infrared (400-3000nm) [10-11]. The semiconductors PbSnSe, PbTe, and PbS, as well as their ternary and quaternary alloys PbSeS, PbSeTe, PbSnSe, and PbSnSeTe, are widely used in a wide range of solid-state mid- and near-infrared devices, including light emitting/detecting devices and thermoelectric generators. IV-VI semiconductor optoelectronic devices, such as laser diodes and photodetectors, are considered more suitable for operating at room temperature due to their two orders of magnitude lower Auger recombination rate compared to II-VI and III-V semiconductors [12].

One of the most critical problems in quantum electronics is the interpretation of experimentally observed quantum confinement effects. This research can help us better understand the quantum physical principles of fundamental quantum effects. The particle in the quantum box is one of the primary and important problems in quantum mechanics, and it is presented in textbooks on basic quantum mechanics. The charge carriers in semiconductors are electrons and holes (excitons). Furthermore, it is well known that reduced dimensionality and quantum size, depending on confinement type (zero, one, or two dimensions), enhance the energy of charge carriers (electron and hole) in semiconductor nanostructures. The size-dependent energy bandgap and wavelength of zero-dimensional semiconductor quantum systems have been studied extensively theoretically [13, 14].

Among the different theoretical models for estimating the energy bandgap and wavelength of semiconductor nanostructures, the cohesive energy model and hyperbolic band model have been used most frequently in the literature [15-17]. Every energy spectrum within a low-dimensional system can be affected by quantum confinement, but not equally. Quantum confinement causes variation in energy bandgap in semiconductors with variation in quantum size, and a blue shift is observed in both absorption and transmission spectrums in all cases. The size of PbSeS nanoparticles has been determined experimentally by SEM, and their energy bandgaps have been determined by Ultra-Violet-NIR and Photoluminescence spectroscopy, and we analyze quantum confinement effects using two known methods (Cohesive energy model and Hyperbolic Band Model). We can estimate the value of energy bandgap and wavelength from these two models and discuss its implications in more detail.

2. Theoretical framework and synthesis of PbSeS QDs

A theoretical framework based on the hyperbolic band model and cohesive energy model has been used to calculate the energy bandgap and wavelength of the QDs. In particular, the surface-volume ratio of semiconductor nanocrystals is essential for analyzing their properties. In semiconductors, Optical and electronic properties are strongly influenced by energy bandgap. Therefore, studying semiconductor nanostructures' variation in energy bandgap is important to understand their better opportunities. All possible electronic transitions can be obtained from the calculated energy bandgap. Energy bandgap is crucial for determining semiconductor properties such as conductivity and wavelength. Semiconductors are primarily used in applications related to the energy bandgap, classified into narrow and wide bandgaps. Materials with narrow bandgaps are used in photosensors and photodetectors, while materials with wide bandgaps are used to manufacture LEDs and laser diodes.

2.1. Hyperbolic band model

It is possible to formulate the hyperbolic model based on two main assumptions. Based on the first approximation, the lowest level of lattice excitation for a binary semiconductor involves the transfer of charge between the metal cation and the anion, which is equivalent to the bulk energy bandgaps of the semiconductor. The second approximation it considers only two bands relevant to the calculation of the energy bandgap; in the Brillouin zone, the bands correspond to the highest levels of occupancy in the valence band and the least amount of occupation in the

conduction band (related to the energy bandgap itself). In most of the analysis Coulomb modifications to the overall energy bandgap shift are considered small, so it is ignored in the present model. In the hyperbolic band model, the size-dependent energy bandgap Eg(QDs) can be calculated analytically using the following formula based on previous assumptions. There may be a significant difference between the L.E. Brus and the hyperbolic model because the holes and electron bands in the hyperbolic band model are not parabolic. The model encompasses electrons and holes behave like hyperbolic bands, but at Brillouin zones, they behave like parabolic bands [15, 16]. As in the hyperbolic band model, electrons' effective mass lies inside the semiconductor and holes' effective mass lies outside. According to Equation (1), the overall shift of energy bandgap depends on the nanomaterial's size by ignoring the Coulomb modifications.

$$E_g(QD) = \sqrt{Eg^2 + \frac{\pi^2 2\,\hbar^2}{m0R^2}\,\frac{1}{2}\,\left(\frac{1}{me^*} + \frac{1}{mh^*}\right)} \tag{1}$$

2.2. Effective mass calculations of electron and hole

An important consideration for ternary alloys is the composition that depends on the effective mass of holes and electrons, energy bandgap, and interband transition energies. A nonlinear relationship between transition energies and alloy composition is examined from the perspective of binary alloy energies and ternary bowing parameters [17]. A ternary alloy's electronic and optical transitions are calculated using interpolation as a function of alloy composition ($0 \leq X \leq 1$). A ternary alloy's composition depends on

$$P_{xyz} = P_{yz} + x\,(P_{xz} - P_{yz}) \tag{2}$$

In order to calculate effective masses for electrons and holes in PbSeS, put the equation as follows:

$$m_{e^*}\ PbSe_xS_{1-x} = m_{e,}\ PbS + X\,(m_{e,}\ PbS - m_{e,}\ PbSe) \tag{3}$$

$$m_{h^*}\ PbSe_xS_{1-x} = m_{h,}\ PbS + X\,(m_{h,}\ PbS - m_{h,}\ PbSe) \tag{4}$$

2.3. Cohesive energy model

Cohesive energy plays a significant role in semiconductor nanomaterials. In order to determine the impact of size-dependent cohesive energies on cluster and free nanoparticles, a theoretical model was developed based on thermodynamic principles. Cohesive energy is the amount of energy required to break all bonds associated with a single molecule within a semiconductor solid. Generally, in nanomaterials, the total cohesive energy is determined by the contribution of atoms on the surface and atoms on the inside, which are given below [18].

$$E_{Total} = E_0\,(n\text{-}N) + (1/2)\,E_0N \tag{5}$$

In the preceding equation, E0 represents the bulk semiconductor's cohesive energy per atom, N represents the number of atoms on the surface, and n indicates the total number of atoms in the nanosolid. (n-N) thus represents the total number of inner atoms in the nanomaterial. As a result, the reference [18] expresses the solution of the aforementioned equation for QDs. The following equation is used to investigate the fluctuation of semiconductor QD bandgap energy as a function of size.

$$E_g\,(D) = E_g\,(bulk)\,(1 + 2d/D) \tag{6}$$

Nanosolids diameter is represented by D and ‘d’ is the diameter of an atom.

3. Parameters for different elements used for PbSeS QDs

The following parameters, which were adapted from the following literature, were used in the work.

Table 1. Different elements' parameters.

Parameters	Values	Literature
Energy bandgap -PbSeS	1.0 eV	20
Electron Effective mass - PbS	0.12 mo	21
Hole Effective mass - PbS	0.11 mo	21
Electron Effective mass -PbSe	0.084 mo	21
Hole Effective mass -PbSe	0.070 mo	21

mo-Mass of electron at rest

4. Synthesis of PbSeS QDs

Using one pot synthesis (hot injection method) under argon atmosphere, $PbSe_xS_{1-x}$ QDs were synthesized under standard vacuum conditions. This is one type of solvothermal method for producing QDs with good stability. Here are the steps involved in the synthesis process: There is a three-neck flask filled with 3 mmol of lead oxide, 7.5 mmol of oleic acid, and 15g of ODE that is degassed under vacuum for 5 minutes, further argon gas is purged into the glass to remove unwanted gas, and the flask is heated under vacuum for 30 minutes to reach a temperature of 100°C. After that, a mixture of 50 g DPP, 1M Se/TOP solution, 50 mg of DPP and 60 mg of TMS2S was injected into the warm solution together with 50 g of DPP. Levels of sulfur and selenium precursors are tuned to specific values, but they're under 1mmol. To dilute the solution, ODE was added after a few seconds. A brown black reaction mixture resulted from the growth of QDs at 100°C for 2 to 3 minutes. Using hexane, purification and separation of QDs were performed, followed by centrifugation and decantation.

5. Results and discussion

The primary objective of this study is to calculate the energy bandgap and wavelength of PbSeS QDs for optoelectronics application. We also examined the QDs' morphological and optical properties.

5.1. UV-Vis-NIR Spectroscopy

Figure 1 illustrates the absorption spectrum of PbSeS semiconductor QDs obtained in the wavelength range of 200 nm to 1600 nm. According to the spectra, the first excitonic peak occurs in the UV range around 240 nm. In accordance with quantum confinement effect, an energy bandgap has been opened and a blue shift has been observed. QDs have a weak absorbance peak that is primarily caused by their non-uniform morphology and dense packing. Generally, QD samples with greater monodispersity show a stronger peak than Nanorod samples. The second peak, which lies in the visible range and around 600 nm, exhibits substantial absorbance. It shows that solar cells are ideally suited to wavelengths within that range. The energy bandgaps of this material range from 5.9eV to 0.82eV based on peak spectrum data analysis. Moreover, the material shows strong absorption in the near-infrared range, which makes it a perfect material for solar cells. It is evident from the UV-VIS-NIR spectrum that there is some absorption at 1359 nm, which is also the most widely used operating wavelength for fibre optic communications.

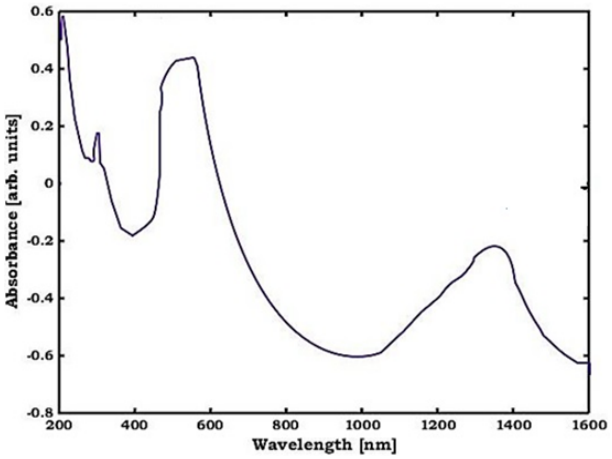

Fig. 1. UV-Vis-NIR absorption spectra PbSeS QDs.

5.2. Photoluminescence spectroscopy

Like the absorbance measurements, photoluminescence spectroscopy was also performed on toluene solutions of PbSeS QDs. As shown in Figure 2, the photoluminescence spectra of PbSeS QDs showed the formation of excitonic peaks in the near-infrared spectrum at 1586 nm, an ideal wavelength for fabricating LEDs and LDs for fiber optic communication sources and solar cell applications.

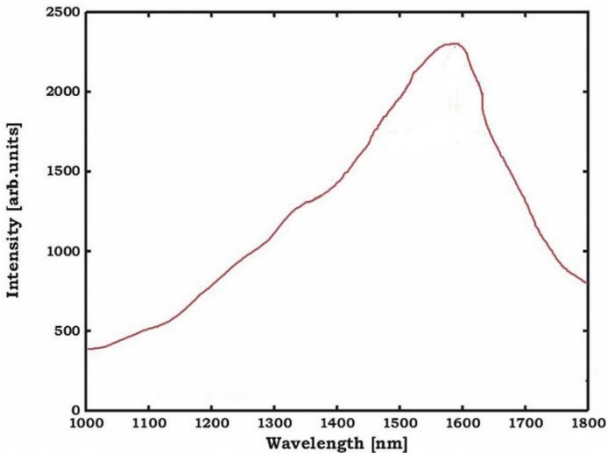

Fig. 2. Photoluminescence spectra of PbSeS QDs.

The commercially preferred wavelengths for fiber optic communications are 850 nm, 1310 nm (O-band), and 1550 nm(C-band). In long distance data transmission applications, C-band is the most commonly used wavelength. The C-band wavelength lends itself well to optical communications due to its low transmission losses. QDs made from PbSeS are easily tuned to achieve this wavelength, making them suitable for producing LEDs, LDs, and photodetectors. There is a possibility of exploitation of solar light at wavelengths ranging from UV to NIR because of the emission peaks in NIR regions.

PbSeS QDs have been found to exhibit a red-shifted in their absorption peaks and their PL peaks. With increasing size, nanocrystals of the Pb chalcogenide group are likely to have significant changes in their energy bandgap due to their large dielectric constants and large excitonic Bohr radius. [22].

5.3. FESEM spectra

FESEM image of PbSeS QDs grown by hot injection method. An image of the prepared material shows visible nano dots. It is evident from the image that QD clusters are dispersed uniformly. Morphological studies suggest that even simple solvothermal methods using hot injection can produce good quality QDs. An average nanodot measures about 8.8nm in diameter.

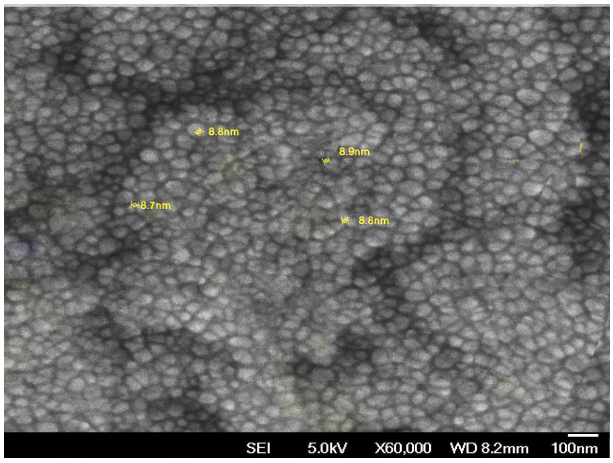

Fig. 3. FESEM of PbSeS QDs.

According to the hyperbolic model and cohesive energy model, this size of QDs has a low energy bandgap. It confirms the efficient growth of QDs and their suitability for optoelectronic device fabrication, in particular solar cells, light-emitting and detecting devices.

5.4. Quantum Size Effects on Energy Bandgap

The results obtained for PbSeS QDs indicate that the energy bandgap depends on the size of the QDs. The energy bandgap of QDs decreases with increasing size, but it never reaches zero. In QDs, an energy bandgap is observed due to an increase in confinement energy level. When the radius of the QDs is comparable to or equal to the exciton Bohr radius and their size is comparable to 2 rB, confinement begins. As the QD size is reduced, the confinement energy level increases until the cluster and magic number of a particular semiconductor material are reached. The energy spectrum in the confinement regime is discrete rather than continuous. Thus, a certain energy level is allowed for a QD of a given size, and at these energies levels, the density of states increases as well. Absorption spectra can be used to observe this experimentally.

Figures 4(a) and 4(b) show spectra probed at different QD sizes. The QDs radius falls below the exciton Bohr radius. There is an increase in the quantum confinement energy as well as an increase in the energy bandgap over the bulk semiconductor material.

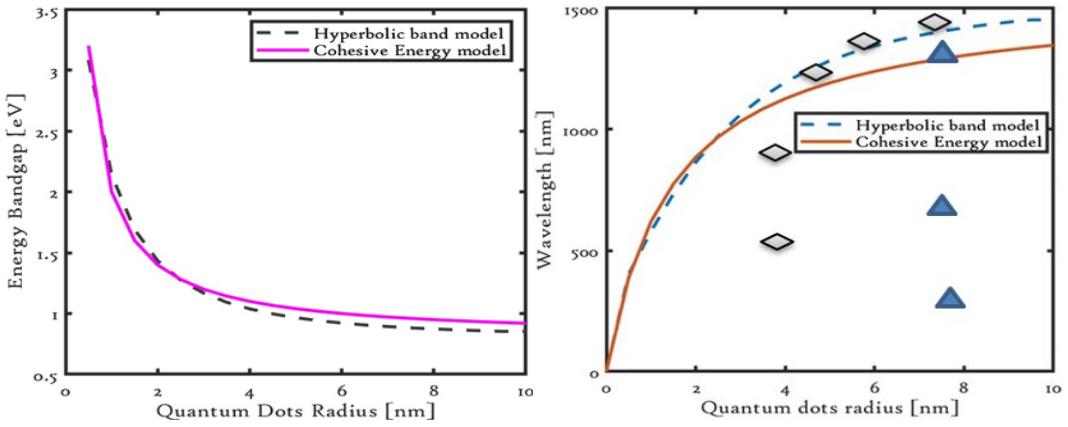

Fig. 4. (a) Size vs. Energy bandgap; (b) Size Vs. wavelength and experimental results marked by solid triangle (our results) and pentagon [23-25].

The cohesive and hyperbolic band models have energy bandgaps of 3.2 eV (402 nm) and 3.08 (387 nm) for QDs with a radius of 0.5 nm. A decrease in energy bandgap is observed as the radius of the QDs approaches 1.1 nm. A close look at this plot reveals when QDs radius is 5-10 nm. There is no considerable variation in quantum dot radius between 3 and 10 nm depending on the QD radius. For the hyperbolic model, the bandgap energy varies between 1.16 eV (1068nm) and 0.85 eV (1458 nm), while for the cohesive model, it varies between 1.2 eV (1033nm) and 0.92 eV (1347 nm). The two models showed the same values, while the QDs ranged in size from 1-3 nm. In this regard, the formula that is used to calculate wavelength is consistent with its exact nature. Ref. [23-25] reports experimental results that are compared with the results obtained in this study. It is reported that the energy bandgap variation follows a similar trend. A good agreement exists between the theory and experimental data for sizes greater than 3 nm. QDs have a large size, their energy levels are so closely spaced that they form a weak confinement region (near continuum) in which electron-hole pairs can be trapped. Due to this, electron-hole pairs in larger-sized QDs have a longer lifespan.

PbSeS quantum dots are most commonly used in solar cells application. The principal source of electrical energy in solar cells is the energy of sunlight. It is estimated that around 50 percentage of sunlight reaches the ground at wavelengths in the visible and UV range, while the remaining portion is in the near infrared and infrared range. Through its visible spectrum, a solar cell converts as much light energy as possible into electrical energy. For maximum current generation at this wavelength, more sun rays are absorbed and more electron-hole pairs are generated. It is possible to achieve this result easily in PbSeS QDs at this wavelength. Further the wavelength can be tunable to achieve near infrared performance to improve the conversion efficiency of solar cells. Further, Optimum tuning of PbSeS QDs was achieved by tuning their wavelength to 1310nm with a 7-8nm radius for both coherent and hyperbolic band models. UV-Vis-NIR results are consistent with predictions. This observation is consistent with the wavelength used in fiber optic communication, i.e., it is a wavelength that is extremely suitable for fabricating laser diodes and LEDs used in fiber optic communication systems. Accordingly, in light of the observations, it is confirmed that the energy band gap of QDs materials has an inverse relationship with wavelength.

Quantum confinement can allow QDs to be tailored to specific levels of incident energy depending on the material's size. As QDs become smaller, their energy bandgap increases and they emit light with a shorter wavelength (blue-shifted). In contrast, as they become more prominent, their energy bandgap decreases, and they emit light with a longer wavelength (red-shifted). A good agreement can be found between theoretical and experimental results.

This confirms the quantum confinement effect in PbSeS material. Some of the predictions in modelling of PbSeS QDs may be of the current interest to researchers engaged in experimental work. Further there is good agreement between predicted experimental works of QDs above 5 nm. This supports correctness of formulation used in this modelling of the nanomaterial.

6. Conclusion

PbSeS QDs were prepared using the hot injection method. UV-Vis-NIR and photoluminescence techniques were used to analyze the optical properties and morphological structures of PbSeS. PbSeS emits infrared wavelengths at 1359 nm with direct energy bandgaps of 0.78 eV. There is a close correlation between experimental data and theoretical results. Furthermore, the PbSeS QDs have significantly improved photovoltaic properties and chemical stability. According to these theoretical models, QDs' energy bandgap decreases as their size increases. To obtain an accurate energy bandgap of semiconductor QDs, effective mass of electrons and holes (m_{e*} & m_{h*}) must be well known. As errors in their values may result in non-negligible errors in the estimation, especially for energies slightly above the bulk bandgap. Regardless of the type of nanoparticle being studied, these considerations must be incorporated into theoretical models.

References

[1] Mukai K., Journal of Nanoscience and Nanotechnology, vol. 14, no. 3, (2014). https://doi.org/10.1166/jnn.2014.8608

[2] Jagannathan, T., Introductory Chapter: The Fame of Quantum Dots in Space-Age Improvements for Multifunctional Application. 18 Jan. 2023; https://doi.org/10.5772/intechopen.108639

[3] Ahamed, M. I., Kumar, K.S., Materials Science- Poland, vol. 37, no. 1, (2019), 108-115; https://doi.org/10.2478/msp-2018-0103

[4] Bawendi, M. G., et al., Physical Review Letters, vol. 65, no. 13, (1990), 1623-1626; https://doi.org/10.1103/PhysRevLett.65.1623

[5] Ekimov, A.I., Onushchenko, A.A., Soviet Journal of Experimental and Theoretical Physics Letters, vol. 34, no. 4, (1981), 345.

[6] Ahamed, M. I., et al., Journal of Ovonic Research, vol. 16, no. 4, (2020), 245-252; https://doi.org/10.15251/JOR.2020.164.245

[7] Ahamed, M.I., Ahamed, M., Muthaiyan, R. (2021), " International Review of Applied Sciences and Engineering, 13(1), pp. 42-46; https://doi.org/10.1556/1848.2021.00288

[8] Ahamed, M. I., Kumar, K.S., Materials Science- Poland, vol. 37, no. 2, (2019), 225-229; https://doi.org/10.2478/msp-2019-0022

[9] Lin, C., et al., International Journal of Molecular Sciences, vol. 12, no. 1, (2011), 476-505; https://doi.org/10.3390/ijms12010476

[10] Brumer, M., et al., Advanced Functional Materials, vol. 15, no. 7, (2005), 1111-1116, https://doi.org/10.1002/adfm.200400620

[11] Pietryga, J.M., et al., Journal of American Chemical Society, vol. 130, no. 14, (2008), 4879-4885; https://doi.org/10.1021/ja710437r

[12] Lifshitz, E., et al., InTech Open, 13 June 2012; https://doi.org/10.5772/35048

[13] Pietryga, Jeffrey M, et al., Journal of American Chemical Society, vol. 130, no. 14, (2008), 4879-4885; https://doi.org/10.1021/ja710437r

[14] Hicks, L. D., et al., Physical Review B, vol. 53, no. 16, (1996), R10493-R10496; https://doi.org/10.1103/PhysRevB.53.R10493

[15] Biljana, P., et al., Journal of Solid State Chemistry, vol. 177, no. 12, (2004), 4785-4799; https://doi.org/10.1016/j.jssc.2004.06.011

[16] Pejova, Biljana, Ivan Grozdanov, Materials Chemistry and Physics, vol. 90, no. 1, (2005), 35-46; https://doi.org/10.1016/j.matchemphys.2004.08.020

[17] Wang, Yang, et al., The Journal of Chemical Physics, vol. 87, no. 12, 15 Dec. 1987, pp. 7315-7322; https://doi.org/10.1063/1.453325

[18] J. Anand, A. Buccheri, M. Gorley, I. Weaver, J. Special Topics, vol. 8, no. 1 (2009).

[19] Ahamed, M. I., et al., Chalcogenide Letters, vol. 18, no. 5, (2021), 245-253; https://doi.org/10.15251/CL.2021.185.245

[20] Midgett, A.G., et al., Nano Letters, vol. 13, no. 7, (2013), 3078-3085; https://doi.org/10.1021/nl4009748

[21] Kang, I., Frank W.W., " Journal of the Optical Society of America B, vol. 14, no. 7, (1997), 1632; https://doi.org/10.1364/JOSAB.14.001632

[22] Wise, F.W., Accounts of Chemical Research, vol. 33, no. 11, (2000), 773-780; https://doi.org/10.1021/ar970220q

[23] Wanli. M., Nano Letter, vol. 9, no.4, (2009), 1699-1703; https://doi.org/10.1021/nl900388a

[24] Minwoo. N., Nanoscale, vol.5, (2013), 8202-8209; https://doi.org/10.1039/c3nr01923c

[25] Guangmei. Z., Nanotechnology, Vol. 23, No. 40, (2012), 405401; https://doi.org/10.1088/0957-4484/23/40/405401